

Adversarial Continual Learning

Sayna Ebrahimi^{1,2}, Franziska Meier¹, Roberto Calandra¹,
Trevor Darrell², and Marcus Rohrbach¹

¹Facebook AI Research, USA ²UC Berkeley EECS, Berkeley, CA, USA
{sayna,trevor}@eecs.berkeley.edu, {fmeier,rcalandra,mrf}@fb.com

Abstract. Continual learning aims to learn new tasks without forgetting previously learned ones. We hypothesize that representations learned to solve each task in a sequence have a shared structure while containing some task-specific properties. We show that shared features are significantly less prone to forgetting and propose a novel hybrid continual learning framework that learns a disjoint representation for task-invariant and task-specific features required to solve a sequence of tasks. Our model combines architecture growth to prevent forgetting of task-specific skills and an experience replay approach to preserve shared skills. We demonstrate our hybrid approach is effective in avoiding forgetting and show it is superior to both architecture-based and memory-based approaches on class incrementally learning of a single dataset as well as a sequence of multiple datasets in image classification. Our code is available at <https://github.com/facebookresearch/Adversarial-Continual-Learning>.

1 Introduction

Humans can learn novel tasks by augmenting core capabilities with new skills learned based on information for a specific novel task. We conjecture that they can leverage a lifetime of previous task experiences in the form of fundamental skills that are robust to different task contexts. When a new task is encountered, these generic strategies form a base set of skills upon which task-specific learning can occur. We would like artificial learning agents to have the ability to solve many tasks sequentially under different conditions by developing task-specific and task-invariant skills that enable them to quickly adapt while avoiding *catastrophic forgetting* [24] using their memory.

One line of continual learning approaches learns a single representation with a fixed capacity in which they detect important weight parameters for each task and minimize their further alteration in favor of learning new tasks. In contrast, structure-based approaches increase the capacity of the network to accommodate new tasks. However, these approaches do not scale well to a large number of tasks if they require a large amount of memory for each task. Another stream of approaches in continual learning relies on explicit or implicit experience replay by storing raw samples or training generative models, respectively. In this paper, we propose a novel adversarial continual learning (ACL) method in which a disjoint latent space representation composed of *task-specific* or *private*

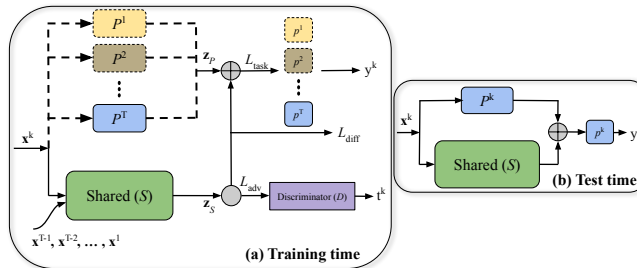


Fig. 1: Factorizing task-specific and task-invariant features in our method (ACL) while learning T sequential tasks at a time. *Left*: Shows ACL at training time where the Shared module is adversarially trained with the discriminator to generate *task-invariant* features (\mathbf{z}_S) while the discriminator attempts to predict task labels. Architecture growth occurs at the arrival of the k^{th} task by adding a *task-specific* modules denoted as P^k and p^k , optimized to generate orthogonal representation \mathbf{z}_P to \mathbf{z}_S to prevent forgetting, 1) Private modules are stored for each task and 2) A shared module which is less prone to forgetting, yet is also retrained with experience reply with a limited number of exemplars *Right*: At test time, the discriminator is removed and ACL uses the P^k module for the specific task it is evaluated on.

latent space is learned for each task and a *task-invariant* or *shared* feature space is learned for all tasks to enhance better knowledge transfer as well as better recall of the previous tasks. The intuition behind our method is that tasks in a sequence share a part of the feature representation but also have a part of the feature representation which is task-specific. The shared features are notably less prone to forgetting and the tasks-specific features are important to retain to avoid forgetting the corresponding task. Therefore, factorizing these features separates the part of the representation that forgets from that which does not forget. To disentangle the features associated with each task, we propose a novel adversarial learning approach to enforce the shared features to be task-invariant and employ orthogonality constraints [30] to enforce the shared features to not appear in the task-specific space.

Once factorization is complete, minimizing forgetting in each space can be handled differently. In the task-specific latent space, due to the importance of these features in recalling the task, we freeze the private module and add a new one upon finishing learning a task. The shared module, however, is significantly less susceptible to forgetting and we only use the replay buffer mechanism in this space to the extent that factorization is not perfect, i.e., when tasks have little overlap or have high domain shift in between, using a tiny memory containing samples stored from prior tasks will help with better factorization and hence higher performance. We empirically found that unlike other memory-based methods in which performance increases by increasing the samples from prior tasks, our model requires a very tiny memory budget beyond which its performance remains constant. This alleviates the need to use old data, as in some applications it might not be possible to store a large amount of data if any at

all. Instead, our approach leaves room for further use of memory, if available and need be, for architecture growth. Our approach is simple yet surprisingly powerful in not forgetting and achieves state-of-the-art results on visual continual learning benchmarks such as MNIST, CIFAR100, Permuted MNIST, miniImageNet, and a sequence of 5 tasks.

2 Related Work

2.1 Continual learning

The existing continual learning approaches can be broadly divided into three categories: memory-based, structure-based, and regularization-based methods.

Memory-based methods: Methods in this category mitigate forgetting by relying on storing previous experience explicitly or implicitly wherein the former raw samples [6,21,28,26,27] are saved into the memory for *rehearsal* whereas in the latter a generative model such as a GAN [32] or an autoencoder [16] synthesizes them to perform *pseudo-rehearsal*. These methods allow for simultaneous multi-task learning on i.i.d. data which can significantly reduce forgetting. A recent study on tiny episodic memories in CL [7] compared methods such as GEM [21], A-GEM [6], MER [27], and ER-RES [7]. Similar to [27], for ER-RES they used reservoir sampling using a single pass through the data. Reservoir sampling [39] is a better sampling strategy for long input data compared to random selection. In this work, we explicitly store raw samples into a very tiny memory used for replay buffer and we differ from prior work by how these stored examples are used by specific parts of our model (discriminator and shared module) to prevent forgetting in the features found to be shared across tasks.

Structure-based methods: These methods exploit modularity and attempt to localize inference to a subset of the network such as columns [29], neurons [11,41], a mask over parameters [23,31]. The performance on previous tasks is preserved by storing the learned module while accommodating new tasks by augmenting the network with new modules. For instance, Progressive Neural Nets (PNNs) [29] statically grow the architecture while retaining lateral connections to previously frozen modules resulting in guaranteed zero forgetting at the price of quadratic scale in the number of parameters. [41] proposed dynamically expandable networks (DEN) in which, network capacity grows according to tasks *relatedness* by splitting/duplicating the most important neurons while time-stamping them so that they remain accessible and re-trainable at all time. This strategy despite introducing computational cost is inevitable in continual learning scenarios where a large number of tasks are to be learned and a fixed capacity cannot be assumed.

Regularization methods: In these methods [18,42,1,25,10], the learning capacity is assumed fixed and continual learning is performed such that the change in parameters is controlled and reduced or prevented if it causes performance downgrade on prior tasks. Therefore, for parameter selection, there has to be defined a *weight importance* measurement concept to prioritize parameter

usage. For instance, inspired by Bayesian learning, in elastic weight consolidation (EWC) method [18] important parameters are those to have the highest in terms of the Fisher information matrix. HAT [31] learns an attention mask over *important* parameters. Authors in [10] used per-weight uncertainty defined in Bayesian neural networks to control the change in parameters. Despite the success gained by these methods in maximizing the usage of a fixed capacity, they are often limited by the number of tasks.

2.2 Adversarial learning

Adversarial learning has been used for different problems such as generative models [13], object composition [2], representation learning [22], domain adaptation [36], active learning [34], etc. The use of an adversarial network enables the model to train in a fully-differentiable manner by adjusting to solve the *minimax* optimization problem [13]. Adversarial learning of the latent space has been extensively researched in domain adaptation [14], active learning [34], and representation learning [17,22]. While previous literature is concerned with the case of modeling single or multiple tasks at once, here we extend this literature by considering the case of continuous learning where multiple tasks need to be learned in a sequential manner.

2.3 Latent Space Factorization

In the machine learning literature, *multi-view* learning, aims at constructing and/or using different views or modalities for better learning performances [3,40]. The approaches to tackle multi-view learning aim at either maximizing the mutual agreement on distinct views of the data or focus on obtaining a latent subspace shared by multiple views by assuming that the input views are generated from this latent subspace using Canonical correlation analysis and clustering [8], Gaussian processes [33], etc. Therefore, the concept of factorizing the latent space into *shared* and *private* parts has been extensively explored for different data modalities. Inspired by the practicality of factorized representation in handling different modalities, here we factorize the latent space learned for different tasks using adversarial learning and orthogonality constraints [30].

3 Adversarial Continual learning (ACL)

We consider the problem of learning a sequence of T data distributions denoted as $\mathcal{D}^{tr} = \{\mathcal{D}_1^{tr}, \dots, \mathcal{D}_T^{tr}\}$, where $\mathcal{D}_k^{tr} = \{(\mathbf{X}_i^k, \mathbf{Y}_i^k, \mathbf{T}_i^k)_{i=1}^{n_k}\}$ is the data distribution for task k with n sample tuples of input ($\mathbf{X}^k \in \mathcal{X}$), output label ($\mathbf{Y}^k \in \mathcal{Y}$), and task label ($\mathbf{T}^k \in \mathcal{T}$). The goal is to sequentially learn the model $f_\theta : \mathcal{X} \rightarrow \mathcal{Y}$ for each task that can map each task input to its target output while maintaining its performance on all prior tasks. We aim to achieve this by learning a disjoint latent space representation composed of a *task-specific* latent space for each task and a *task-invariant* feature space for all tasks to enhance better knowledge transfer as

well as better catastrophic forgetting avoidance of prior knowledge. We mitigate catastrophic forgetting in each space differently. For the *task-invariant* feature space, we assume a limited memory budget of \mathcal{M}^k which stores m samples $x_{i=1\dots m} \sim \mathcal{D}_{j=1\dots k-1}^{tr}$ from every single task prior to k .

We begin by learning f_{θ}^k as a mapping from \mathbf{X}^k to \mathbf{Y}^k . For C -way classification task with a cross-entropy loss, this corresponds to

$$\mathcal{L}_{\text{task}}(f_{\theta}^k, \mathbf{X}^k, \mathbf{Y}^k, \mathcal{M}^k) = -\mathbb{E}_{(x^k, y^k) \sim (\mathbf{X}^k, \mathbf{Y}^k) \cup \mathcal{M}^k} \sum_{c=1}^C \mathbb{1}_{[c=y^k]} \log(\sigma(f_{\theta}^k(x^k))) \quad (1)$$

where σ is the softmax function and the subscript $i = \{1, \dots, n_t\}$ is dropped for simplicity. In the process of learning a sequence of tasks, an ideal f^k is a model that maps the inputs to two independent latent spaces where one contains the shared features among all tasks and the other remains private to each task. In particular, we would like to disentangle the latent space into the information shared across all tasks (\mathbf{z}_S) and the independent or private information of each task (\mathbf{z}_P) which are as distinct as possible while their concatenation followed by a task-specific head outputs the desired targets.

To this end, we introduce a mapping called Shared ($S_{\theta_S} : \mathcal{X} \rightarrow \mathbf{z}_S$) and train it to generate features that fool an adversarial discriminator D . Conversely, the adversarial discriminator ($D_{\theta_D} : \mathbf{z}_S \rightarrow \mathcal{T}$) attempts to classify the generated features by their task labels ($\mathbf{T}^{k \in \{0, \dots, T\}}$). This is achieved when the discriminator is trained to maximize the probability of assigning the correct task label to generated features while simultaneously S is trained to confuse the discriminator by minimizing $\log(D(S(x^k)))$. This corresponds to the following T -way classification cross-entropy adversarial loss for this minimax game

$$\mathcal{L}_{\text{adv}}(D, S, \mathbf{X}^k, \mathbf{T}^k, \mathcal{M}^k) = \min_S \max_D \sum_{k=0}^T \mathbb{1}_{[k=t^k]} \log(D(S(x^k))) . \quad (2)$$

Note that the extra label zero is associated with the ‘fake’ task label paired with randomly generated noise features of $\mathbf{z}'_S \sim \mathcal{N}(\mu, \Sigma)$. In particular, we use adversarial learning in a different regime that appears in most works related to generative adversarial networks [13] such that the generative modeling of input data distributions is not utilized here because the ultimate task is to learn a discriminative representation.

To facilitate training S , we use the Gradient Reversal layer [12] that optimizes the mapping to maximize the discriminator loss directly ($\mathcal{L}_{\text{task}_S} = -\mathcal{L}_D$). In fact, it acts as an identity function during forward propagation but negates its inputs and reverses the gradients during back propagation. The training for S and D is complete when S is able to generate features that D can no longer predict the correct task label for leading \mathbf{z}_S to become as task-invariant as possible. The private module ($P_{\theta_P} : \mathcal{X} \rightarrow \mathbf{z}_P$), however, attempts to accommodate the task-invariant features by learning merely the features that are specific to the task in hand and do not exist in \mathbf{z}_S . We further factorize \mathbf{z}_S and \mathbf{z}_P by using

orthogonality constraints introduced in [30], also known as “difference” loss in the domain adaptation literature [4], to prevent the shared features between all tasks from appearing in the private encoded features. This corresponds to

$$\mathcal{L}_{\text{diff}}(S, P, \mathbf{X}^k, \mathcal{M}^k) = \sum_{k=1}^T \|(S(x^k))^T P^k(x^k)\|_F^2, \quad (3)$$

where $\|\cdot\|_F$ is the Frobenius norm and it is summed over the encoded features of all P modules encoding samples for the current tasks and the memory.

Final output predictions for each task are then predicted using a task-specific multi-layer perceptron head which takes \mathbf{z}_P concatenated with \mathbf{z}_S ($\mathbf{z}_P \oplus \mathbf{z}_S$) as an input. Taken together, these loss form the complete objective for ACL as

$$\mathcal{L}_{\text{ACL}} = \lambda_1 \mathcal{L}_{\text{adv}} + \lambda_2 \mathcal{L}_{\text{task}} + \lambda_3 \mathcal{L}_{\text{diff}}, \quad (4)$$

where λ_1 , λ_2 , and λ_3 are regularizers to control the effect of each component. The full algorithm for ACL is given in Alg. 1.

3.1 Avoiding forgetting in ACL

Catastrophic forgetting occurs when a representation learned through a sequence of tasks changes in favor of learning the current task resulting in performance downgrade on previous tasks. The main insight to our approach is decoupling the conventional *single* representation learned for a sequence of tasks into two parts: a part that *must not change* because it contains task-specific features without which complete performance retrieval is not possible, and a part that is *less prone to change* as it contains the core structure of all tasks.

To *fully prevent* catastrophic forgetting in the first part (private features), we use *compact* modules that can be stored into memory. If factorization is successfully performed, the second part remains highly immune to forgetting. However, we empirically found that when disentanglement cannot be fully accomplished either because of the little overlap or large domain shift between the tasks, using a tiny replay buffer containing few samples for old data can be beneficial to retain high ACC values as well as mitigating forgetting.

3.2 Evaluation metrics

After training for each new task, we evaluate the resulting model on all prior tasks. Similar to [21,10], to measure ACL performance we use ACC as the average test classification accuracy across all tasks. To measure forgetting we report backward transfer, BWT, which indicates how much learning new tasks has influenced the performance on previous tasks. While $\text{BWT} < 0$ directly reports *catastrophic forgetting*, $\text{BWT} > 0$ indicates that learning new tasks has helped with the preceding tasks.

$$\text{BWT} = \frac{1}{T-1} \sum_{i=1}^{T-1} R_{T,i} - R_{i,i}, \quad \text{ACC} = \frac{1}{T} \sum_{i=1}^T R_{T,i} \quad (5)$$

Algorithm 1 Adversarial Continual Learning (ACL)

```

1: function TRAIN( $\theta_P, \theta_S, \theta_D, \mathcal{D}^{tr}, \mathcal{D}^{ts}, m$ )
2:   Hyper-parameters:  $\lambda_1, \lambda_2, \lambda_3, \alpha_S, \alpha_P, \alpha_D$ 
3:    $R \leftarrow 0 \in \mathbb{R}^{T \times T}$ 
4:    $\mathcal{M} \leftarrow \{\}$ 
5:    $f_\theta^k = f(\theta_S \oplus \theta_P)$ 
6:   for  $k = 1$  to  $T$  do
7:     for  $e = 1$  to epochs do
8:       Compute  $\mathcal{L}_{adv}$  for  $S$  using  $(x, t) \in \mathcal{D}_k^{tr} \cup \mathcal{M}$ 
9:       Compute  $\mathcal{L}_{task}$  using  $(x, y) \in \mathcal{D}_k^{tr} \cup \mathcal{M}$ 
10:      Compute  $\mathcal{L}_{diff}$  using  $P^k, S$ , and  $x \in \mathcal{D}_k^{tr}$ 
11:       $\mathcal{L}_{ACL} = \lambda_1 \mathcal{L}_{adv} + \lambda_2 \mathcal{L}_{task} + \lambda_3 \mathcal{L}_{diff}$ 
12:       $\theta'_S \leftarrow \theta_S - \alpha_S \nabla \mathcal{L}_{ACL}$ 
13:       $\theta'_{P_t} \leftarrow \theta_{P^k} - \alpha_{P^k} \nabla \mathcal{L}_{ACL}$ 
14:      Compute  $\mathcal{L}_{adv}$  for  $D$  using  $(S(x), t)$ 
        and  $(\mathbf{z}' \sim \mathcal{N}(\mu, \Sigma), t = 0)$ 
15:       $\theta'_D \leftarrow \theta_D - \alpha_D \nabla \mathcal{L}_{adv}$ 
16:    end for
17:     $\mathcal{M} \leftarrow \text{UPDATEMEMORY}(\mathcal{D}_k^{tr}, \mathcal{M}, C, m)$ 
18:    Store  $\theta_{P^k}$ 
19:     $f_\theta^k \leftarrow f(\theta'_S \oplus \theta'_{P_t})$ 
20:     $R_{k, \{1 \dots k\}} \leftarrow \text{EVAL}(f_\theta^k, \mathcal{D}_{\{1 \dots k\}}^{ts})$ 
21:  end for
22: end function

function UPDATEMEMORY( $\mathcal{D}_k^{tr}, \mathcal{M}, C, m$ )
   $s \leftarrow \frac{m}{C} \triangleright s := \#$  of samples per class
  for  $c = 1$  to  $C$  do
    for  $i = 1$  to  $n$  do
       $(x_i^k, y_i^k, t_i^k) \sim \mathcal{D}_k^{tr}$ 
       $\mathcal{M} \leftarrow \mathcal{M} \cup (x_i^k, y_i^k, t_i^k)$ 
    end for
  end for
  return  $\mathcal{M}$ 
end function

function EVAL( $f_\theta^k, \mathcal{D}_{\{1 \dots k\}}^{ts}$ )
  for  $i = 1$  to  $k$  do
     $R_{k,i} = \text{Accuracy}(f_\theta^k(x, t), y)$  for  $(x, y, t) \in \mathcal{D}_i^{ts}$ 
  end for
  return  $R$ 
end function

```

where $R_{n,i}$ is the test classification accuracy on task i after sequentially finishing learning the n^{th} task. We also compare methods based on the memory used either in the network architecture growth or replay buffer. Therefore, we convert them into memory size assuming numbers are 32-bit floating point which is equivalent to 4bytes.

4 Experiments

In this section, we review the benchmark datasets and baselines used in our evaluation as well as the implementation details.

4.1 ACL on Vision Benchmarks

Datasets: We evaluate our approach on the commonly used benchmark datasets for T -split class-incremental learning where the entire dataset is divided into T disjoint subsets or tasks. We use common image classification datasets including **5-Split MNIST** and **Permuted MNIST** [20], previously used in [25,42,10], **20-Split CIFAR100** [19] used in [42,21,6], and **20-Split miniImageNet** [38] used in [7,43]. We also benchmark ACL on a sequence of **5-Datasets** including **SVHN**, **CIFAR10**, **not-MNIST**, **Fashion-MNIST** and, **MNIST** and report average performance over multiple random task orderings. Dataset statistics are

given in Table 4a in the appendix. No data augmentation of any kind has been used in our analysis.

Baselines: From the prior work, we compare with state-of-the-art approaches in all the three categories described in Section 2 including Elastic Weight Consolidation (EWC) [18], Progressive neural networks (PNNs) [29], and Hard Attention Mask (HAT) [31] using implementations provided by [31] unless otherwise stated. For memory-based methods including A-GEM, GEM, and ER-RES, for Permuted MNIST, 20-Split CIFAR100, and 20-Split miniImageNet, we relied on the implementation provided by [7], but changed the experimental setting from single to multi-epoch and without using 3 Tasks for cross-validation for a more fair comparison against ACL and other baselines. On Permuted MNIST results for SI [42] are reported from [31], for VCL [25] those are obtained using their original provided code, and for Uncertainty-based CL in Bayesian framework (UCB) [10] are directly reported from the paper. We also perform fine-tuning, and joint training. In fine-tuning (ORD-FT), an ordinary single module network without the discriminator is continuously trained without any forgetting avoidance strategy in the form of experience replay or architecture growth. In joint training with an ordinary network (ORD-JT) and our ACL setup (ACL-JT) we learn all the tasks jointly in a multitask learning fashion using the entire dataset at once which serves as the upper bound for average accuracy on all tasks, as it does not adhere to the continual learning scenario.

Implementation details: For all ACL experiments except for Permuted MNIST and 5-Split MNIST we used a reduced AlexNet [15] architecture as the backbone for S and P modules for a fair comparison with the majority of our baselines. However, ACL can be also used with more sophisticated architectures (see our code repository for implementation of ACL with reduced ResNet18 backbone). However, throughout this paper, we only report our results using AlexNet. The architecture in S is composed of 3 convolutional and 4 fully-connected (FC) layers whereas P is only a convolutional neural network (CNN) with similar number of layers and half-sized kernels compared to those used in S . The private head modules (p) and the discriminator are all composed of a small 3-layer perceptron. Due to the differences between the structure of our setup and a regular network with a single module, we used a similar CNN structure to S followed by larger hidden FC layers to match the total number of parameters throughout our experiments with our baselines for fair comparisons. For 5-Split MNIST and Permuted MNIST where baselines use a two-layer perceptron with 256 units in each and ReLU nonlinearity, we used a two-layer perceptron of size 784×175 and 175×128 with ReLU activation in between in the shared module and a single-layer of size 784×128 and ReLU for each P . In each head, we also used an MLP with layers of size 256 and 28, ReLU activations, and a 14-unit softmax layer. In all our experiments, no pre-trained model is used. We used stochastic gradient descent in a multi-epoch setting for ACL and all the baselines.

5 Results and Discussion

In the first set of experiments, we measure ACC, BWT, and the memory used by ACL and compare it against state-of-the-art methods with or without memory constraints on 20-Split miniImageNet. Next, we provide more insight and discussion on ACL and its component by performing an ablation study and visualizations on this dataset. In Section 6, we evaluate ACL on a more difficult continual learning setting where we sequentially train on 5 different datasets. Finally, in section (7), we demonstrate the experiments on sequentially learning single datasets such as 20-Split CIFAR100 and MNIST variants.

5.1 ACL Performance on 20-Split miniImageNet

Starting with 20-Split miniImageNet, we split it in 20 tasks with 5 classes at a time. Table 1a shows our results obtained for ACL compared to several baselines. We compare ACL with HAT as a regularization based method with no experience replay memory dependency that achieves $ACC=59.45 \pm 0.05$ with $BWT=-0.04 \pm 0.03\%$. Results for the memory-based methods of ER-RES and A-GEM are re(produced) by us using the implementation provided in [7] by applying modifications to the network architecture to match with ACL in the backbone structure as well as the number of parameters. We only include A-GEM in Table 1a which is only a faster algorithm compared to its precedent GEM with identical performance. A-GEM and ER-RES use an architecture with 25.6M parameters (102.6MB) along with storing 13 images of size $(84 \times 84 \times 3)$ per class (110.1MB) resulting in total memory size of 212.7MB. ACL is able to outperform all baselines in $ACC=62.07 \pm 0.51$, $BWT=0.00 \pm 0.00$, using total memory of 121.6MB for architecture growth (113.1MB) and storing 1 sample per class for replay buffer (8.5MB). In our ablation study in Section 5.2, we will show our performance without using replay buffer for this dataset is $ACC=57.66 \pm 1.44$. However, ACL is able to overcome the gap by using only one image per class (5 per task) to achieve $ACC=62.07 \pm 0.51$ without the need to have a large buffer for old data in learning datasets like miniImagenet with diverse sets of classes.

5.2 Ablation Studies on 20-Split miniImageNet

We now analyze the major building blocks of our proposed framework including the discriminator, the shared module, the private modules, replay buffer, and the *difference* loss on the miniImagenet dataset. We have performed a complete cumulative ablation study for which the results are summarized in Table 1b and are described as follows:

Shared and private modules: Using only a shared module without any other ACL component (ablation #1 in Table 1b) yields the lowest ACC of 21.19 ± 4.43 as well as the lowest BWT performance of -60.10 ± 4.14 while using merely private modules (ablation #2) obtains a slightly better ACC of 29.05 ± 5.67 and a zero-guaranteed forgetting by definition. However, in both scenarios the ACC

Table 1: CL results on 20-Split miniImageNet measuring ACC (%), BWT (%), and Memory (MB). (**) denotes that methods do not adhere to the continual learning setup: ACL-JT and ORD-JT serve as the upper bound for ACC for ACL/ORD networks, respectively. (*) denotes result is re(produced) by us using the original provided code. (†) denotes result is obtained using the re-implementation setup by [31]. BWT of Zero indicates the method is zero-forgetting guaranteed. (b) Cumulative ablation study of ACL on miniImageNet where P : private modules, S : shared module, D : discriminator, $\mathcal{L}_{\text{diff}}$: orthogonality constraint, and RB: replay buffer memory of one sample per class. All results are averaged over 3 runs and standard deviation is given in parentheses

(a)					(b)							
Method	ACC%	BWT%	Arch (MB)	Replay Buffer (MB)	#	S	P	D	$\mathcal{L}_{\text{diff}}$	RB	ACC%	BWT%
HAT* [31]	59.45(0.05)	-0.04(0.03)	123.6	-	1	x					21.19(4.43)	-60.10(4.14)
PNN † [29]	58.96(3.50)	Zero	588	-	2		x				29.09(5.67)	Zero
ER-RES* [7]	57.32(2.56)	-11.34(2.32)	102.6	110.1	3	x		x			32.82(2.71)	-28.67(3.61)
A-GEM* [6]	52.43(3.10)	-15.23(1.45)	102.6	110.1	4	x	x		x		49.13(3.45)	-3.99(0.42)
ORD-FT	28.76(4.56)	-64.23(3.32)	37.6	-	5	x	x				50.15(1.41)	-14.32(2.34)
ORD-JT**	69.56(0.78)	-	5100	-	6	x	x			x	51.19(1.98)	-9.12(2.98)
ACL-JT**	66.89(0.32)	-	5100	-	7	x	x		x	x	52.07(2.49)	-0.01(0.01)
ACL (Ours)	62.07(0.51)	0.00(0.00)	113.1	8.5	8	x	x	x			55.72(1.42)	-0.12(0.34)
					9	x	x	x	x		57.66(1.44)	-3.71(1.31)
					10	x	x	x		x	60.28(0.52)	0.00(0.00)
					11	x	x	x	x	x	62.07(0.51)	0.00(0.00)

Table 2: Comparison of the effect of the replay buffer size between ACL and other baselines including A-GEM [6], and ER-RES [7] on 20-Split miniImageNet where unlike the baselines, ACL’s performance remains unaffected by the increase in number of samples stored per class as discussed in 5.2. The results from this table are used to generate Fig. 3 in the appendix.

Samples per class	1	3	5	13
A-GEM[6]	45.14(3.42)	49.12(4.69)	50.24(4.56)	52.43(3.10)
ER-RES[7]	40.21(2.68)	46.87(4.51)	53.45(3.45)	57.32(2.56)
ACL (ours) ACC	62.07(0.51)	61.80(0.50)	61.69(0.61)	61.33(0.40)
BWT	0.00(0.00)	0.01(0.00)	0.01(0.00)	-0.01(0.02)

achieved is too low considering the random chance being 20% which is due to the small size of networks used in S and P .

Discriminator and orthogonality constraint ($\mathcal{L}_{\text{diff}}$): The role of adversarial training or presence of D on top of S and P can be seen by comparing the ablations #8 and #5 where in the latter D , as the only disentanglement mechanism, is eliminated. We observe that ACC is improved from 50.15 ± 1.41 to $55.72 \pm 1.42\%$ and BWT is increased from -14.32 ± 2.34 to $-0.12 \pm 0.34\%$. On the other hand, the effect of orthogonality constraint as the only factorization mechanism is shown in ablation #4 where the $\mathcal{L}_{\text{diff}}$ can not improve the ACC performance, but it increases BWT form -14.32 ± 2.34 to -3.99 ± 0.42 . Comparing ablations #8 and #4 shows the importance of adversarial training in factorizing the latent spaces versus orthogonality constraint if they were to be used individually. To compare the role of adversarial and diff losses in the presence of replay buffer (RB), we can compare #7 and #10 in which the D and $\mathcal{L}_{\text{diff}}$ are ablated, respectively. It appears again that D improves ACC more than $\mathcal{L}_{\text{diff}}$ by reaching $\text{ACC}=60.28 \pm 0.52$ whereas $\mathcal{L}_{\text{diff}}$ can only achieve $\text{ACC}=52.07 \pm 2.49$. However, the effect of D and $\mathcal{L}_{\text{diff}}$ on BWT is nearly the same.

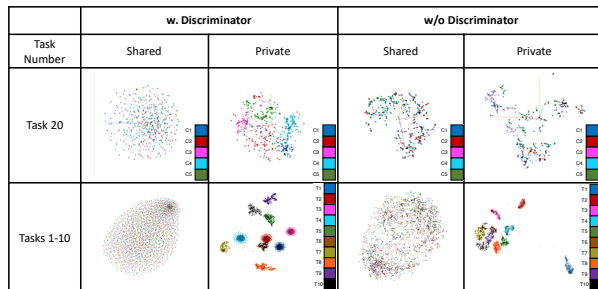


Fig. 2: Visualizing the effect of adversarial learning on the latent space generated by shared and private modules on 20-Split miniImageNet.

Replay buffer: Here we explore the effect of adding the smallest possible memory replay to ACL, i. e., storing one sample per class for each task. Comparing ablation #9 and the most complete version of ACL (#11) shows that adding this memory improves both the ACC and BWT by 4.41% and 3.71%, respectively. We also evaluated ACL using more samples in the memory. Table 2 shows that unlike A-GEM and ER-RES approaches in which performance increases with more episodic memory, in ACL, ACC remains nearly similar to its highest performance. Being insensitive to the amount of old data is a remarkable feature of ACL, not because of the small memory it consumes, but mainly due to the fact that access to the old data might be prohibited or very limited in some real-world applications. Therefore, for a fixed allowed memory size, a method that can effectively use it for architecture growth can be considered as more practical for such applications.

5.3 Visualizing the effect of adversarial learning in ACL

Here we illustrate the role of adversarial learning in factorizing the latent space learned for continually learning a sequence of tasks using the t-distributed Stochastic Neighbor Embedding (t-SNE) [37] plots for the 20-Split miniImageNet experiment. The depicted results are obtained without using the orthogonality constraint, ($\mathcal{L}_{\text{diff}}$), to merely present the role of adversarial learning.

Fig. 2 visualizes the latent spaces of the shared and private modules trained with and without the discriminator. In the first row, we used the model trained on the entire sequence of 20-Split miniImageNet and evaluated it on the test-sets belonging to task #20 including 100 images for 5 classes, a total of 500 samples, which are color-coded with their class labels. In the second row, once again we used our final model trained on the entire sequence of 20-Split miniImageNet and tested it on the first 10 tasks of the sequence one at a time and plotted them all in a single figure for both shared and private modules with and without the discriminator where samples are color-coded with their task labels.

We first compare the discriminator’s effect on the latent space generated by the shared modules (second column). The shared modules trained with adver-

serial loss, consistently appear as a uniformly mixed distribution of encoded samples both for task #20 and the first 10 tasks. In contrast, in the generated features without a discriminator in the fourth column for task #20, we observe a non-uniformly distributed mixture of features where small clusters can be found for some classes showing an entangled representation within each task. Similar to the pattern for task #20, we observe a mixed latent space representing the shared space for the first 10 tasks (fourth column).

The effect of the discriminator on the private modules’ latent spaces is shown in the third and fifth columns where in the former, private modules trained with a discriminator, appear to be nearly successful in uncovering class labels (first row) and task labels (second row), although the final classification is yet to be happening in the private heads. As opposed to that, in the absence of the discriminator, private modules generate features as entangled as those generated by their shared module counterparts (first row). Private modules of the first 10 tasks is not as well-clustered as the private module trained with discriminator. As we can see in the fifth column, features for task #6 are spread into two parts with one close to task #7 and the other next to task #9.

6 ACL Performance on a sequence of 5-Datasets

In this section, we present our results for continual learning of 5 tasks using ACL in Table 3b. Similar to the previous experiment we look at both ACC and BWT obtained for ACL, finetuning as well as UCB as our baseline. Results for this sequence are averaged over 5 random permutations of tasks and standard deviations are given in parenthesis. CL on a sequence of datasets has been previously performed by two regularization based approaches of UCB and HAT where UCB was shown to be superior [10]. With this given sequence, ACL is able to outperform UCB by reaching $ACC=78.55(\pm 0.29)$ and $BWT=-0.01$ using only half of the memory size and also no replay buffer. In Bayesian neural networks such as UCB, there exists double number of parameters compared to a regular model representing mean and variance of network weights. It is very encouraging to see that ACL is not only able to continually learn on a single dataset, but also across diverse datasets.

7 Additional Experiments

20-Split CIFAR100: In this experiment we incrementally learn CIFAR100 in 5 classes at a time in 20 tasks. As shown in Table 3, HAT is the most competitive baseline, although it does not depend on memory and uses 27.2MB to store its architecture in which it learns task-based attention maps reaching $ACC=76.96 \pm 1.23\%$. PNN uses 74.7MB to store the lateral modules to the memory and guarantees zero forgetting. Results for A-GEM, and ER-Reservoir are re(produced) by us using a CNN similar to our shared module architecture. We use fully connected layers with more number of neurons to compensate for the remaining number of parameters reaching 25.4MB of memory. We also

Table 3: CL results on 20-Split CIFAR100 measuring ACC (%), BWT (%), and Memory (MB). (**) denotes that methods do not adhere to the continual learning setup: ACL-JT and ORD-JT serve as the upper bound for ACC for ACL/ORD networks, respectively. (*) denotes result is obtained by using the original provided code. (†) denotes result is obtained using the re-implementation setup by [31]. (°) denotes result is reported by [7]. BWT of Zero indicates the method is zero-forgetting guaranteed. All results are averaged over 3 runs and standard deviation is given in parentheses.

(a) 20-Split CIFAR100					(b) Sequence of 5 Datasets				
Method	ACC%	BWT%	Arch (MB)	Replay Buffer (MB)	Method	ACC%	BWT%	Arch (MB)	Replay Buffer (MB)
HAT * [31]	76.96(1.23)	0.01(0.02)	27.2	-	UCB * [10]	76.34(0.12)	-1.34(0.04)	32.8	-
PNN† [29]	75.25(0.04)	Zero	93.51	-	ORD-FT	27.32(2.41)	-42.12(2.57)	16.5	-
A-GEM° [6]	54.38(3.84)	-21.99(4.05)	25.4	16	ACL (Ours)	78.55(0.29)	-0.01(0.15)	16.5	-
ER-RES° [7]	66.78(0.48)	-15.01(1.11)	25.4	16					
ORD-FT	34.71(3.36)	-48.56(3.17)	27.2	-					
ORD-JT**	78.67(0.34)	-	764.5	-					
ACL-JT**	79.91(0.05)	-	762.6	-					
ACL (Ours)	78.08(1.25)	0.00(0.01)	25.1	-					

stored 13 images per class (1300 images of size $(32 \times 32 \times 3)$ in total) which requires 16.0MB of memory. However, ACL achieves ACC= $(78.08 \pm 1.25)\%$ with BWT= $0.00 \pm 0.01\%$ using only 25.1MB to grow private modules with 167.2K parameters (0.6MB) without using memory for replay buffer which is mainly due to the overuse of parameters for CIFAR100 which is considered as a relevantly ‘easy’ dataset with all tasks (classes) sharing the same data distribution. Disentangling shared and private latent spaces, prevents ACL from using redundant parameters by only storing task-specific parameters in P and p modules. In fact, as opposed to other memory-based methods, instead of starting from a large network and using memory to store samples, which might not be available in practice due to confidentiality issues (*e.g.* medical data), ACL uses memory to gradually add small modules to accommodate new tasks and relies on knowledge transfer through the learned shared module. The latter is what makes ACL to be different than architecture-based methods such as PNN where the network grows by the entire *column* which results in using a highly disproportionate memory to what is needed to learn a new task with.

Permuted MNIST: Another popular variant of the MNIST dataset in CL literature is Permuted MNIST where each task is composed of randomly permuting pixels of the entire MNIST dataset. To compare against values reported in prior work, we particularly report on a sequence of $T = 10$ and $T = 20$ tasks with ACC, BWT, and memory for ACL and baselines. To further evaluate ACL’s ability in handling more tasks, we continually learned up to 40 tasks. As shown in Table 5 in the appendix, among the regularization-based methods, HAT achieves the highest performance of 91.6% [31] using an architecture of size 1.1MB. Vanilla VCL improves by 7% in ACC and 6.5% in BWT using a K-means core-set memory size of 200 samples per task (6.3MB) and an architecture size similar to HAT. PNN appears as a strong baseline achieving ACC=93.5% with guaranteed

zero forgetting. Finetuning (ORD-FT) and joint training (ORD-JT) results for an ordinary network, similar to EWC and HAT (a two-layer MLP with 256 units and ReLU activations), are also reported as reference values for lowest BWT and highest achievable ACC, respectively. ACL achieves the highest accuracy among all baselines for both sequences of 10 and 20 equal to $\text{ACC}=98.03 \pm 0.01$ and $\text{ACC}=97.81 \pm 0.03$, and $\text{BWT}=-0.01\%$ $\text{BWT}=0\%$, respectively which shows that performance of ACL drops only by 0.2% as the number of tasks doubles. ACL also remains efficient in using memory to grow the architecture compactly by adding only 55K parameters (0.2MB) for each task resulting in using a total of 2.4MB and 5.0MB when $T = 10$ and $T = 20$, respectively for the entire network including the shared module and the discriminator. We also observed that the performance of our model does not change as the number of tasks increases to 30 and 40 if each new task is accommodated with a new private module. We did not store old data and used memory only to grow the architecture by 55K parameters (0.2MB).

5-Split MNIST: As the last experiment in this section, we continually learn 0–9 MNIST digits by following the conventional pattern of learning 2 classes over 5 sequential tasks [25,42,10]. As shown in Table 6 in the appendix, we compare ACL with regularization-based methods with no memory dependency (EWC, HAT, UCB, Vanilla VCL) and methods relying on memory only (GEM), and VCL with K-means Core-set (VCL-C) where 40 samples are stored per task. ACL reaches $\text{ACC}=(\mathbf{99.76} \pm \mathbf{0.03})\%$ with zero forgetting outperforming UCB with $\text{ACC}=99.63\%$ which uses nearly 40% more memory size. In this task, we only use architecture growth (no experience replay) where 54.3K private parameters are added for each task resulting in memory requirement of 1.6MB to store all private modules. Our core architecture has a total number of parameters of 420.1K. We also provide naive finetuning results for ACL and a regular single-module network with (268K) parameters (1.1MB). Joint training results for the regular network (ORD-JT) is computed as $\text{ACC}=99.89 \pm 0.01$ for ACL which requires 189.3MB for the entire dataset as well as the architecture.

8 Conclusion

In this work, we proposed a novel hybrid continual learning algorithm that factorizes the representation learned for a sequence of tasks into *task-specific* and *task-invariant* features where the former is important to be fully preserved to avoid forgetting and the latter is empirically found to be remarkably less prone to forgetting. The novelty of our work is that we use adversarial learning along with orthogonality constraints to disentangle the shared and private latent representations which results in compact private modules that can be stored into memory and hence, efficiently preventing forgetting. A tiny replay buffer, although not critical, can be also integrated into our approach if forgetting occurs in the shared module. We established a new state of the art on CL benchmark datasets.

References

1. Aljundi, R., Babiloni, F., Elhoseiny, M., Rohrbach, M., Tuytelaars, T.: Memory aware synapses: Learning what (not) to forget. In: Proceedings of the European Conference on Computer Vision (ECCV). pp. 139–154 (2018)
2. Azadi, S., Pathak, D., Ebrahimi, S., Darrell, T.: Compositional gan: Learning image-conditional binary composition. *International Journal of Computer Vision* pp. 1–16 (2020)
3. Blum, A., Mitchell, T.: Combining labeled and unlabeled data with co-training. In: Proceedings of the eleventh annual conference on Computational learning theory. pp. 92–100. ACM (1998)
4. Bousmalis, K., Trigeorgis, G., Silberman, N., Krishnan, D., Erhan, D.: Domain separation networks. In: Advances in neural information processing systems. pp. 343–351 (2016)
5. Chaudhry, A., Dokania, P.K., Ajanthan, T., Torr, P.H.: Riemannian walk for incremental learning: Understanding forgetting and intransigence. In: Proceedings of the European Conference on Computer Vision (ECCV). pp. 532–547 (2018)
6. Chaudhry, A., Ranzato, M., Rohrbach, M., Elhoseiny, M.: Efficient lifelong learning with A-GEM. In: International Conference on Learning Representations (2019)
7. Chaudhry, A., Rohrbach, M., Elhoseiny, M., Ajanthan, T., Dokania, P.K., Torr, P.H., Ranzato, M.: Continual learning with tiny episodic memories. arXiv preprint arXiv:1902.10486 (2019)
8. Chaudhuri, K., Kakade, S.M., Livescu, K., Sridharan, K.: Multi-view clustering via canonical correlation analysis. In: Proceedings of the 26th annual international conference on machine learning. pp. 129–136. ACM (2009)
9. Deng, J., Dong, W., Socher, R., Li, L.J., Li, K., Fei-Fei, L.: ImageNet: A Large-Scale Hierarchical Image Database. In: CVPR09 (2009)
10. Ebrahimi, S., Elhoseiny, M., Darrell, T., Rohrbach, M.: Uncertainty-guided continual learning with bayesian neural networks. In: International Conference on Learning Representations (2020)
11. Fernando, C., Banarse, D., Blundell, C., Zwols, Y., Ha, D., Rusu, A.A., Pritzel, A., Wierstra, D.: Pathnet: Evolution channels gradient descent in super neural networks. arXiv preprint arXiv:1701.08734 (2017)
12. Ganin, Y., Ustinova, E., Ajakan, H., Germain, P., Larochelle, H., Laviolette, F., Marchand, M., Lempitsky, V.: Domain-adversarial training of neural networks. *The Journal of Machine Learning Research* **17**(1), 2096–2030 (2016)
13. Goodfellow, I., Pouget-Abadie, J., Mirza, M., Xu, B., Warde-Farley, D., Ozair, S., Courville, A., Bengio, Y.: Generative adversarial nets. In: Advances in neural information processing systems. pp. 2672–2680 (2014)
14. Hoffman, J., Tzeng, E., Park, T., Zhu, J.Y., Isola, P., Saenko, K., Efros, A., Darrell, T.: CyCADA: Cycle-consistent adversarial domain adaptation. In: International Conference on Machine Learning. pp. 1989–1998 (2018)
15. Iandola, F.N., Han, S., Moskewicz, M.W., Ashraf, K., Dally, W.J., Keutzer, K.: Squeezenet: Alexnet-level accuracy with 50x fewer parameters and < 0.5 mb model size. arXiv preprint arXiv:1602.07360 (2016)
16. Kemker, R., Kanan, C.: Fearnnet: Brain-inspired model for incremental learning. In: International Conference on Learning Representations (2018)
17. Kim, H., Mnih, A.: Disentangling by factorising. arXiv preprint arXiv:1802.05983 (2018)

18. Kirkpatrick, J., Pascanu, R., Rabinowitz, N., Veness, J., Desjardins, G., Rusu, A.A., Milan, K., Quan, J., Ramalho, T., Grabska-Barwinska, A., et al.: Overcoming catastrophic forgetting in neural networks. *Proceedings of the national academy of sciences* p. 201611835 (2017)
19. Krizhevsky, A., Hinton, G.: Learning multiple layers of features from tiny images. *Tech. rep., Citeseer* (2009)
20. LeCun, Y., Bottou, L., Bengio, Y., Haffner, P.: Gradient-based learning applied to document recognition. *Proceedings of the IEEE* **86**(11), 2278–2324 (1998)
21. Lopez-Paz, D., et al.: Gradient episodic memory for continual learning. In: *Advances in Neural Information Processing Systems*. pp. 6467–6476 (2017)
22. Makhzani, A., Shlens, J., Jaitly, N., Goodfellow, I., Frey, B.: Adversarial autoencoders. *arXiv preprint arXiv:1511.05644* (2015)
23. Mallya, A., Lazebnik, S.: Packnet: Adding multiple tasks to a single network by iterative pruning. In: *IEEE Conference on Computer Vision and Pattern Recognition (CVPR)* (2018)
24. McCloskey, M., Cohen, N.J.: Catastrophic interference in connectionist networks: The sequential learning problem. In: *Psychology of learning and motivation*, vol. 24, pp. 109–165. Elsevier (1989)
25. Nguyen, C.V., Li, Y., Bui, T.D., Turner, R.E.: Variational continual learning. In: *ICLR* (2018)
26. Rebuffi, S.A., Kolesnikov, A., Sperl, G., Lampert, C.H.: icarl: Incremental classifier and representation learning. In: *CVPR* (2017)
27. Riemer, M., Cases, I., Ajemian, R., Liu, M., Rish, I., Tu, Y., , Tesauro, G.: Learning to learn without forgetting by maximizing transfer and minimizing interference. In: *International Conference on Learning Representations* (2019)
28. Robins, A.: Catastrophic forgetting, rehearsal and pseudorehearsal. *Connection Science* **7**(2), 123–146 (1995)
29. Rusu, A.A., Rabinowitz, N.C., Desjardins, G., Soyer, H., Kirkpatrick, J., Kavukcuoglu, K., Pascanu, R., Hadsell, R.: Progressive neural networks. *arXiv preprint arXiv:1606.04671* (2016)
30. Salzman, M., Ek, C.H., Urtasun, R., Darrell, T.: Factorized orthogonal latent spaces. In: *Proceedings of the Thirteenth International Conference on Artificial Intelligence and Statistics*. pp. 701–708 (2010)
31. Serra, J., Suris, D., Miron, M., Karatzoglou, A.: Overcoming catastrophic forgetting with hard attention to the task. In: Dy, J., Krause, A. (eds.) *Proceedings of the 35th International Conference on Machine Learning. Proceedings of Machine Learning Research*, vol. 80, pp. 4548–4557. PMLR (2018)
32. Shin, H., Lee, J.K., Kim, J., Kim, J.: Continual learning with deep generative replay. In: *Advances in Neural Information Processing Systems*. pp. 2990–2999 (2017)
33. Shon, A., Grochow, K., Hertzmann, A., Rao, R.P.: Learning shared latent structure for image synthesis and robotic imitation. In: *Advances in neural information processing systems*. pp. 1233–1240 (2006)
34. Sinha, S., Ebrahimi, S., Darrell, T.: Variational adversarial active learning. In: *Proceedings of the IEEE International Conference on Computer Vision*. pp. 5972–5981 (2019)
35. Srivastava, R.K., Masci, J., Kazerounian, S., Gomez, F., Schmidhuber, J.: Compete to compute. In: *Advances in neural information processing systems*. pp. 2310–2318 (2013)

36. Tzeng, E., Hoffman, J., Saenko, K., Darrell, T.: Adversarial discriminative domain adaptation. In: Proceedings of the IEEE Conference on Computer Vision and Pattern Recognition. pp. 7167–7176 (2017)
37. Van Der Maaten, L.: Accelerating t-sne using tree-based algorithms. *The Journal of Machine Learning Research* **15**(1), 3221–3245 (2014)
38. Vinyals, O., Blundell, C., Lillicrap, T., Wierstra, D., et al.: Matching networks for one shot learning. In: Advances in neural information processing systems. pp. 3630–3638 (2016)
39. Vitter, J.S.: Random sampling with a reservoir. *ACM Transactions on Mathematical Software (TOMS)* **11**(1), 37–57 (1985)
40. Xu, C., Tao, D., Xu, C.: A survey on multi-view learning. arXiv preprint arXiv:1304.5634 (2013)
41. Yoon, J., Yang, E., Lee, J., Hwang, S.J.: Lifelong learning with dynamically expandable networks. In: International Conference on Learning Representations (2018)
42. Zenke, F., Poole, B., Ganguli, S.: Continual learning through synaptic intelligence. In: Precup, D., Teh, Y.W. (eds.) Proceedings of the 34th International Conference on Machine Learning. Proceedings of Machine Learning Research, vol. 70, pp. 3987–3995. PMLR (2017)
43. Zhang, M., Wang, T., Lim, J.H., Feng, J.: Prototype reminding for continual learning. arXiv preprint arXiv:1905.09447 (2019)

Adversarial Continual Learning

(Supplementary Materials)

Sayna Ebrahimi^{1,2}, Franziska Meier¹, Roberto Calandra¹,
Trevor Darrell², Marcus Rohrbach¹
Facebook AI Research, Menlo Park, USA
UC Berkeley EECS, Berkeley, CA, USA

9 Datasets

Table 4a shows a summary of the datasets utilized in our work. From left to right columns are given as: dataset name, total number of classes in the dataset, number of tasks, image size, number of training images per task, number of validation images per task, number of test images per task, and number of classes in each task. Statistic of 5-Split MNIST and 5-Datasets experiments are given in 4b and 4c, respectively. We did not use data augmentation for any dataset.

(a) Statistics of utilized datasets

Dataset	#Classes	#Tasks	Input Size	#Train/Task	#Valid/Task	#Test/Task	#Class/Task
5-Split MNIST [20]	10	5	$1 \times 28 \times 28$	10	see Tab. 4b	see Tab. 4b	2
Permuted MNIST [35]	10	10/20/30/40	$1 \times 28 \times 28$	51,000	9,000	10,000	10
20-Split CIFAR100 [19]	100	20	$3 \times 32 \times 32$	2,125	375	500	5
20-Split miniImageNet [9]	100	20	$3 \times 84 \times 84$	2,125	375	500	5
5-Datasets	5×10	5	$3 \times 32 \times 32$	see Tab. 4c	see Tab. 4c	see Tab. 4c	10

(b) Number of training, validation, and test samples per task for 5-Split MNIST

Task number	T = 1 (0,1)	T=2 (2,3)	T=3 (4,5)	T=4 (6,7)	T=5 (8,9)
# Training samples	10766	10276	9574	10356	10030
# Validation samples	1899	1813	1689	1827	1770
# Test samples	2115	2042	1874	1986	1983

(c) Statistics of utilized datasets in 5-Datasets. MNIST, notMNIST, and Fashion MNIST are padded with 0 to become 32×32 and have 3 channels.

Dataset	MNIST	notMNIST	Fashion MNIST	CIFAR10	SVHN
# Training samples	51,000	15,526	9,574	42,500	62,269
# Validation samples	9,000	2,739	1,689	7,500	10,988
# Test samples	10,000	459	1,874	10,000	26,032

10 Results on Permuted MNIST and 5-Split MNIST

Table 5 and 6 show results obtained for Permuted MNIST and 5-Split MNIST experiments described in section 7, respectively.

11 Effect of memory size on ACL

Fig. 3 shows the effect of memory size on ACL and memory-dependent baselines when 1, 3, 5, and 13 images per class are used during training where in the left

Table 5: CL results on Permuted MNIST. measuring ACC (%), BWT (%), and Memory (MB). (**) denotes that methods do not adhere to the continual learning setup: ACL-JT and ORD-JT serve as the upper bound for ACC for ACL/ORD networks, respectively. (*) denotes result is obtained by using the original provided code. (‡) denotes result reported from original work. (°) denotes the results reported by [7] and (°°) denotes results are reported by [31]; T shows the number of tasks. Note the difference between BWT of Zero and 0.00 where the former indicates the method is zero-forgetting guaranteed by definition and the latter is computed using Eq. 5. All results are averaged over 3 runs, the standard deviation is provided in parenthesis.

Method	ACC%	BWT%	Arch Buffer (MB)	Replay Buffer (MB)
EWC ^{°°} [18] (T=10)	88.2	-	1.1	-
HAT [‡] [31] (T=10)	97.4	-	2.8	-
UCB [‡] [10] (T=10)	91.44(0.04)	-0.38(0.02)	2.2	-
VCL* [25] (T=10)	88.80(0.23)	-7.90(0.23)	1.1	-
VCL-C* [25](T=10)	95.79(0.10)	-1.38(0.12)	1.1	6.3
PNN [°] [29] (T=20)	93.5(0.07)	Zero	N/A	-
ORD-FT (T=10)	44.91(6.61)	-53.69(1.91)	1.1	-
ORD-JT** (T=10)	96.03(0.02)	-	189.3	-
ACL-JT** (T=10)	98.45(0.02)	-	194.4	-
ACL (Ours) (T=10)	98.03(0.01)	-0.01(0.01)	2.4	-
ACL (Ours) (T=20)	97.81(0.03)	0.00(0.00)	5.0	-
ACL (Ours) (T=30)	97.81(0.03)	0.00(0.00)	7.2	-
ACL (Ours) (T=40)	97.80(0.02)	0.00(0.00)	9.4	-

it illustrates the memory effect for ACL and memory-dependent baselines. We also show how memory affects the BWT in ACL in Fig. 3 (right) which follows the same pattern as we observed for ACC. Numbers used to plot this figure with their standard deviation are given in Table 2.

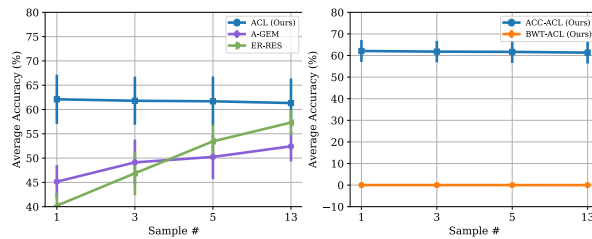


Fig. 3: *Left*: Comparing the replay buffer effect on ACC on 20-Split miniImageNet achieved by ACL against A-GEM [6] and ER-RES [7] when using 1, 3, 5, and 13 samples per classes within each task discussed in 5.2. *Right*: Insensitivity of ACC and BWT to replay buffer in ACL. Best viewed in color.

Table 6: Class Incremental Learning on 5-Split MNIST. measuring ACC (%), BWT (%), and Memory (MB). (**) denotes that methods do not adhere to the continual learning setup: ACL-JT and ORD-JT serve as the upper bound for ACC for ACL/ORD networks, respectively. (*) denotes result is obtained by using the original provided code. (‡) denotes result reported from original work and (††) denotes results are reported by [10]; All results are averaged over 3 runs, the standard deviation is provided in parenthesis

Method	ACC%	BWT%	Arch (MB)	Replay Buffer (MB)
EWC †† [18]	95.78(0.35)	-4.20(0.21)	1.1	-
HAT †† [31]	99.59(0.01)	0.00(0.04)	1.1	-
UCB ‡ [10]	99.63(0.02)	0.00(0.00)	2.2	-
VCL * [25]	95.97(1.03)	-4.62(1.28)	1.1	-
GEM* [21]	94.34(0.82)	-2.01(0.05)	6.5	0.63
VCL-C * [25]	93.6(0.20)	-3.10(0.20)	1.7	0.63
ORD-FT	65.96(3.53)	-40.15(4.27)	1.1	-
ORD-JT**	99.88(0.02)	-	189.3	-
ACL-JT** (Ours)	99.89(0.01)	-	190.8	-
ACL (Ours)	99.76(0.03)	0.01(0.01)	1.6	-

12 Intransigence Measure

Table 7 shows our results for Intransigence (I) measure introduced in [5] and computed for the k -th task as below:

$$I_k = a_k^* - a_{k,k} \quad (6)$$

where a_k^* is the accuracy on the k -th task using a reference model trained with all the seen datasets up to task k and $a_{k,k}$ denotes the accuracy on the k -th task when trained up to task k in an incremental manner. $I_k \in [-1, 1]$.

Table 7 shows I evaluated at the end of tasks sequence for ACL and the strongest baselines (HAT [31] and ER-RES) in 5-Split MNIST, Permuted MNIST, 20-Split CIFAR100, and 20-Split miniImageNet experiments. We found ACL achieves the lowest I (lower the better) value compared to baselines, always negative, which means in ACL, learning tasks up to a specific task in hand increases the model’s ability to learn new ones which is consistent with our idea of proposing a shared latent space for better initialization for new tasks.

Table 7: Intransigence measure results obtained for 5-Split MNIST, Permuted MNIST, 20-Split CIFAR100, and 20-Split miniImageNet experiments in HAT [31], ER-RES, and ACL. I_k denotes the measure computed at the end of the k -th task.

	5-Split MNIST (I_5)	Permuted MNIST (I_{10})	20-Split CIFAR100 (I_{20})	20-Split miniImageNet (I_{20})
HAT [31]	-0.0001	-0.01	0.1	0.1
ER-RES	0.002	0.001	-0.002	-0.02
ACL (Ours)	-0.5	-0.04	-0.03	-0.2